Jan Heitmann, Fabian Steinmetz, and Christian Renner. A Case for Chirp Modulation for Low-Power Acoustic Communication in Shallow Waters. In Proc. of the 17th GI/ITG KuVS Fachgespräch Sensornetze, FGSN'18, Braunschweig, Germany, Sept. 2018.

A Case for Chirp Modulation for Low-Power Acoustic Communication in Shallow Waters

Jan Heitmann, Fabian Steinmetz, Christian Renner
Research Group smartPORT
Hamburg University of Technology
Email: {jheitmann, fabian.steinmetz, christian.renner}@tuhh.de

***Abstract*—Small and cheap micro AUVs enable diverse underwater monitoring applications in shallow inshore waters; e.g., inspection of underwater assets, observation of water quality, and identification of pollution sources. The formation and collaboration of swarm members yet requires communication and self-localization based on cheap, miniature acoustic devices. However, this is severely hampered by the effects of multi-path propagation in shallow waters. We study the benefits and applicability of narrow-band chirp-based modulation vs. frequency-shift keying (FSK). First, we discuss the influence of multi-path propagation on FSK through real-world experiments. Second, we show that narrow-band chirps can be used as a direct replacement of FSK symbols, increasing the detection probability by up to 23% and accuracy and precision by up to 39% and 53%, respectively, at virtually no bandwidth penalty.**

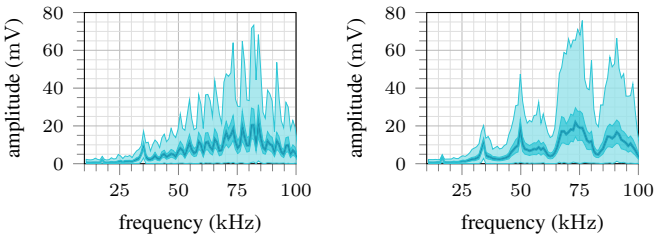

Fig. 1: Quartiles of received frequency shares of a 1 s band-limited (10 kHz to 100 kHz) pseudo-random acoustic signal at 2.1 m (left) and 5.1 m (right). Received signals were sampled at 1 MHz and broken into 976 segments of 1024 samples each. Sender and receiver were submerged ∼0.5 m in LOS conditions in a marina in Hamburg.

I. Introduction

Exploration and monitoring of underwater sceneries is drawing considerable attention. Recent examples are the investigation of sub-mesoscale eddies [1] or ship tracking in harbors [2]. Timely acquisition of data mandates communication—typically wireless to keep installation and maintenance cost low. Acoustic underwater modems have been proposed by academia [3], [4] and launched by industry [5]–[7] for this purpose.

Shallow and relatively small water bodies—such as port basins, lakes, or canals—are a particularly challenging scenery. Reflections at the water surface cause massive inter- and intra-symbol interference, because the non-line-of-sight (NLOS) signals have a low delay and attenuation only [8]. In previous research [3] and recent measurement campaigns, we experienced significant attenuation and amplification of frequency shares depending on position and time. Figure 1 indicates the frequency selectivity of the acoustic channel. In addition, we noted influence of environmental conditions and their change over time. Proposed countermeasures are, e.g., frequency hopping, PSK, and OFDM [9], [10]. Unfortunately, inshore applications and the implied use of μAUVs mandates miniature, low-power modems such as [3] with low computing power and resources that are insufficient to run such algorithms.

We embark on a different strategy, namely the use of narrow-band chirp signals for preamble-based synchronization, motivated by the following observations. We noted that communication with our acoustic modem was—despite using FSK modulation—reliable, if the preamble was successfully detected by the receiver. Failure to do so arises mainly from cancellation and amplification caused by reflections and scattering. The main reason for this is intra-symbol interference leading to unreliable symbol detection and hence synchronization. Once the synchronization has succeeded, however, the symbol windows are known and reliable communication can be achieved through relatively simple methods such as frequency hopping and redundancy coding.

We make the following contributions: We motivate the benefit of narrow-band chirp modulation for preamble-based synchronization. We sketch a low-complexity implementation for low-power acoustic modems. We evaluate our approach against two non-coherent detection and cross-correlation for FSK modulation. Our results are based on real-world experiments in conditions similar to typical inshore, shallow-water application scenarios.

II. Fundamentals

A. Frequency-Shift Keying

Frequency-Shift Keying (FSK) is commonly used in acoustic underwater communication. In binary frequency-shift keying (BFSK), a bit b is transmitted as a sinusoidal symbol with frequency f_b and duration T. There are more complex forms of FSK, which we do not address in detail due to space constraints.

Receivers often employ non-coherent detection due to its efficiency, but cross-correlation is also possible. Orthogonal frequencies f_b may improve detection. The (envelope) shape of detector output is trapezoidal for undistorted symbols with constant amplitude, with its peak marking the symbol's end. If reflections overlap with the line-of-sight (LOS) signal, detector

output contains overlapping triangles as in Figs. 2a and 2b. Depending on the number and phase of reflections, a clear peak is no longer present, impacting detection accuracy and likelihood.

B. Chirp Keying

A chirp is a signal with steadily changing frequency over time. We consider linear chirps, where the frequency sweeps linearly over time from frequency f_s to f_e. The chirp has duration T and bandwidth $B = |f_e - f_s|$. A bandwidth-efficient way to employ binary modulation is to use down-chirps ($f_s > f_e$) and up-chirps ($f_s < f_e$) to represent bit b.

Detection of a chirp can be achieved through cross-correlation. The detector output is a narrow and steep peak, which allows a clear distinction between the LOS signal and reflected signals as displayed in Fig. 2c. Because of this property, chirps are commonly employed in radar applications. For a given T, B can be chosen such that up- and down-chirp are orthogonal, or vice versa.

C. Comparison and Discussion

In various real-world experiments (cf. Fig. 1 and [3]), we confirmed heavy, time-varying, and location-dependent frequency selectivity of the acoustic channel. This is of paramount relevance for preamble-based synchronization. Here, symbol (window) positions are derived by detecting the preamble symbols or their peaks, respectively. For successful packet reception and precise time-of-flight ranging [11], accurate synchronization is mandatory. In case of FSK, signal cancellation and reverberation due to reflections cause poor synchronization. As shown in Fig. 2, the peak of the originally trapezoidal detection result is blurred and accurate detection hampered. Noise and multiple echos aggravate this situation. In case of destructive interference, a peak may not be found at all.

Chirp modulation brings two advantages: (i) its frequency spreading increases detection probability, because attenuation of frequency shares due to reflection is drastically reduced, and (ii) the peaks of the LOS signal and its echos are separable in the time domain, so that a smaller synchronization error is expected. Using chirps yet comes at a cost. The benefit of non-coherent FSK detection is its low computation complexity. For each new sample, two multiplications are required, giving a constant computation complexity per new sample. Without optimization, cross-correlation has to be performed for a full symbol for every sample, yielding at least logarithmic computation complexity per new sample. For low-power acoustic modems, this complexity may already be infeasible. Hence, we study the performance of chirp vs. FSK in general but also discuss the feasibility of chirp detection on low-power acoustic modems.

III. Preamble-Based Synchronization

Preamble-based synchronization is achieved through a preamble of N_{pre} symbols of alternating up- and down-chirps followed by a start frame delimiter (SFD) of N_{sfd} symbols.

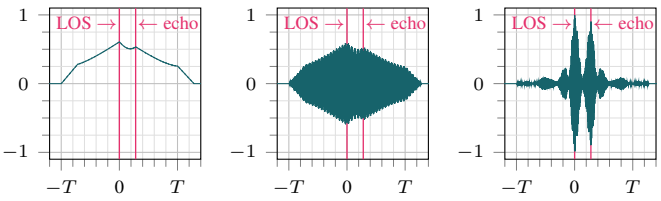

(a) FSK non-coherent (b) FSK cross-corr. (c) chirp cross-corr.

Fig. 2: Detection of chirp ($f_s = 50\,\text{kHz}$, $f_e = 54\,\text{kHz}$) and FSK ($f = 50\,\text{kHz}$) signal superimposed by an echo with 0.7 ms delay and 90% amplitude (ca. 10 m distance at 2 m depth). Symbol duration is $T = 2.5\,\text{ms}$. Time on the x-axis is relative to perfect LOS detection.

To detect the presence of a synchronization sequence, the receiver employs a signal level threshold τ. The reason for this approach is that continuous cross-correlation for each new sample is typically infeasible on low-power modems.

To detect the first preamble symbol after threshold exceedance, a cross-correlation over a window of length $2T$ is calculated. We chose twice the symbol duration to obtain an extended window to search for correlation peaks. The highest peak is accepted as valid preamble symbol, if its value exceeds the mean of the correlation values by a factor of ρ. After detection of the first peak, windows of length $(1+\alpha)T$ $(0 < \alpha < 2)$ in steps of T relative to the first symbol (peak) are used to detect the remaining preamble symbols. Note that factor α sets the size and overlap of the search windows of the individual symbols and marks a trade-off between calculation speed and detection tolerance. When the SFD sequence is identified, we take the median of all stored detection times, delete all synchronization symbols with a deviation of more than βT $(0 < \beta < 1)$. The mean value of the remaining peaks' times is finally accepted as synchronization point—i.e., the symbols of the following data packet are expected in intervals of T relative to this time.

Based on previous finding and dedicated experiments, we chose $N_{\text{pre}} = 16$ and $N_{\text{sfd}} = 4$, $\alpha = 0.4$, $\tau = 20\%$, $\rho = 3$, and $\beta = 0.1$.

IV. Experimentation Setup

For all experiments, we used the smartPORT acoustic modem [3], a low-power, low-cost device for use in μAUVs such as MONSUN [12] and Hippocampus [13]. The required amount of signal processing limits the sampling frequency to 200 kHz. The receive circuitry embraces an analog 16^{th}-order bandpass filter with passband from 50 kHz to 75 kHz and a digitally-adjustable gain. The communication range is above 100 m with an Aquarian Audio AS-1 hydrophone as transducer.

For evaluation of our chirp-based synchronization, we conducted real-world tests in the marina of TuS Finkenwerder, which offers ideal and realistic testing conditions: Several jetties of up to 150 m length allow for testing at versatile distances and in LOS conditions. This plot resembles the envisioned scenario in rivers and port basins. The water is at least 2 m deep.

Due to the fundamental nature of our investigation, signal preparation and processing was done with MATLAB. Signal generation and recording was performed with a TiePie HS5 USB oscilloscope and waveform generator connected to the receiver and the transmitter circuitry of our acoustic modem. Sender and receiver were connected to the same oscilloscope to enable calculation of absolute time differences. Cable lengths limited the maximum distance to $5.1\,\mathrm{m}$.

Unless stated otherwise, the sampling rate of the receiver was $200\,\mathrm{kHz}$ to match the setting of our modem. Hydrophones were placed in a depth of ca. $0.5\,\mathrm{m}$. To obtain a ground-truth for synchronization accuracy, we sent a long, wide-band chirp ($10\,\mathrm{kHz}$ to $150\,\mathrm{kHz}$, $100\,\mathrm{ms}$) sampled with $1\,\mathrm{MHz}$. For each distance, this measurement was repeated 10 times, producing a reference value with a standard deviation of at most $2.1\,\mu\mathrm{s}$.

V. Results

A. Synchronization Macroscope

First, we evaluated chirp vs. FSK synchronization on a wide frequency band of $40\,\mathrm{kHz}$ to $90\,\mathrm{kHz}$ with frequency steps of $2\,\mathrm{kHz}$. The distance between sender and receiver was $5.1\,\mathrm{m}$. We performed 100 synchronization attempts per modulation scheme and frequency with $T = 2.5\,\mathrm{ms}$ and $B = 2.342\,\mathrm{kHz}$, which produces orthogonal up- and down-chirps. We examined synchronization accuracy and precision in terms of the mean and standard deviation of the absolute synchronization errors. Besides the LOS signal, we observed a dominant (surface) reflection arriving with a mean delay of $54\,\mu\mathrm{s}$ (cf. Sect. IV).

Figure 3 shows heatmaps of the synchronization errors. The figure reveals high variance for non-coherent (Fig. 3a) and cross-correlation (Fig. 3b) FSK; i.e., lower precision compared to chirps (Fig. 3c). Only in rare cases, the benefit of chirp modulation is small—e.g., for $f = 90\,\mathrm{kHz}$, precision is lower than for FSK; and for $f = 46\,\mathrm{kHz}$, its benefit is marginal.

An important aspect of synchronization is the percentile of successful detection within a given margin of a symbol duration T, because this will affect the number of bit errors during demodulation of the transmitted data packet; e.g., a 10% margin means that the actual symbol and demodulation window overlap by 90%. According to our measurements, chirping achieves 83.8% vs. 76.8% and 67.9% for cross-correlation and non-coherent FSK, respectively, for a margin of 10% (or $250\,\mu\mathrm{s}$). This implies a 23% improvement of chirping over non-coherent FSK. For a 20% margin, these numbers climb up to ∼90% for all modulation schemes.

Regarding accuracy and precision, chirping outperforms non-coherent FSK with an average synchronization error of $56.5\,\mu\mathrm{s}$ vs. $93.1\,\mu\mathrm{s}$ and a standard deviation of $39.9\,\mu\mathrm{s}$ vs. $84.9\,\mu\mathrm{s}$ for a 10% margin. Surprisingly, cross-correlation FSK has better (average) accuracy ($34.5\,\mu\mathrm{s}$) but lower precision ($99.0\,\mu\mathrm{s}$). Figure 3b shows many early synchronizations, which are caused by received signal cancellation due to reflections. In case of chirping, on the contrary, there is a tendency to late detection caused by the surface reflection. In addition to accuracy, we also calculated absolute synchronization errors, because from a perspective of succesful packet reception, negative and positive errors do not cancel out from packet to packet. The corresponding numbers are $75.2\,\mu\mathrm{s}$ for chirp, $106.3\,\mu\mathrm{s}$ for cross-correlation, and $119.9\,\mu\mathrm{s}$ for non-coherent FSK, exhibiting a 29.3% advantage of chirping. Values for a 20% margin are comparable and omitted.

B. Synchronization Microscope

We further explored the previous findings by examining the distribution of synchronization times for one frequency band in detail. For this experiment, 1000 synchronization sequences have been sent for each modulation scheme and at distances of $2.1\,\mathrm{m}$ and $5.1\,\mathrm{m}$. We used $f_0 = 62.44\,\mathrm{kHz}$, $f_1 = 62.84\,\mathrm{kHz}$ for FSK and $f_\mathrm{s} = 62.44\,\mathrm{kHz}$, $f_\mathrm{e} = 64.782\,\mathrm{kHz}$ for chirping.

Figure 4 shows the distribution of synchronization errors. At a distance of $2.1\,\mathrm{m}$, chirping has a $13.7\,\%$ higher success rate compared to FSK, whereas the improvement of accuracy and precision is small. However, at a distance of $5.1\,\mathrm{m}$ (Figs. 4a to 4c), chirp synchronization improves overall success rate of up to $20.7\,\%$ and also accuracy and precision are improved. The reason for this is that at larger distances, LOS and NLOS (surface reflection) signals exhibit less separation in time-domain. Figure 5 provides a detailed study of our performance metrics, and it shows that chirping improves the synchronization precision up to factor of 3.1. It is also evident that chirping elevates the success rate considerable and provides higher accuracy.

VI. Conclusion

Underwater communication and self-localization are required for the deployment of swarms of μAUVs. Preamble-based synchronization for communication is hampered due to reflections in shallow waters. We showed that chirp modulation for synchronization is generally superior to FSK modulation, as it improves accuracy, precision, and success rate. This enables higher data rates, less packet loss, and better (packet-based) localization accuracy. We experienced that the benefit of using chirp synchronization is larger at a distance of $5.1\,\mathrm{m}$ than at $2.1\,\mathrm{m}$. We expect that this also holds for much larger distances, because the relative error between LOS signal and first echo decreases at large distances. However, chirp detection is more complex and needs carefully designed algorithms and implementations for low-power acoustic modems.

Acknowledgment

This work has been partially supported by the German Federal Ministry of Education and Research (BMBF, FKZ 13N14153), the German Federal Ministry for Economic Affairs and Energy (BMWi, FKZ 03SX463C), and ERA-NET Cofund MarTERA (contract 728053). The authors would like to thank Lucas Bublitz for building acoustic modems and TuS Finkenwerder for granting access to their jetties and facilities.

References

[1] B. Meyer, C. Isokeit, E. Maehle, and B. Baschek, "Using Small Swarm-Capable AUVs for Submesoscale Eddy Measurements in the Baltic Sea," in *Proc. of the MTS/IEEE Oceans Conf.*, Sep. 2017.

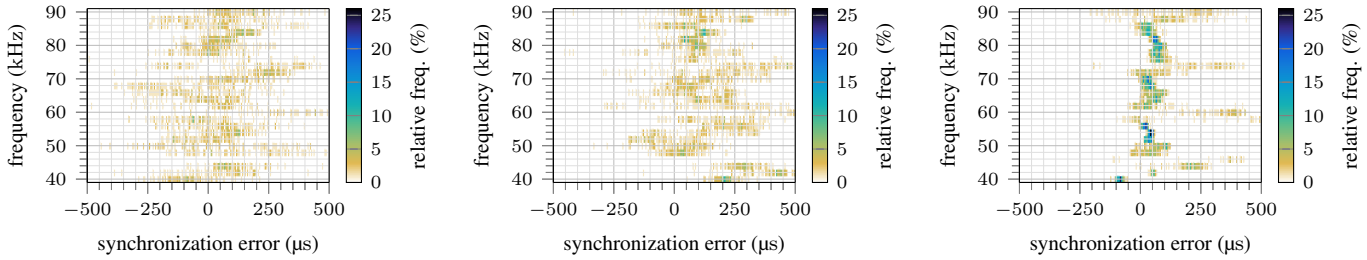

(a) FSK, non-coherent detector (b) FSK, cross-correlation (c) Chirp, cross-correlation

Fig. 3: Heatmaps of synchronization errors for chirp and FSK-based synchronization and 5.1 m LOS distance. Time resolution is 5 µs.

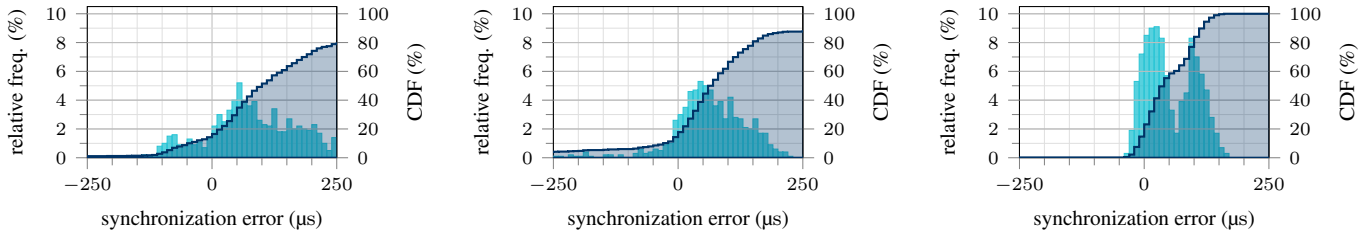

(a) FSK, non-coherent detector, 5.1 m dist. (b) FSK, cross-correlation, 5.1 m dist. (c) chirp, cross-correlation, 5.1 m dist.

Fig. 4: Distribution and cumulative distribution function (CDF) of synchronization errors for chirp and FSK based synchronization ($f_0 = 62.44\,\text{kHz}$, $f_1 = 62.84\,\text{kHz}$, $f_s = 62.44\,\text{kHz}$, $f_e = 64.782\,\text{kHz}$). Turquoise graphs show the relative distribution, blue line the cumulative frequencies. Failed synchronizations or this with an error of more than $\pm 250\,\mu\text{s}$ are not included in the plot for better readability.

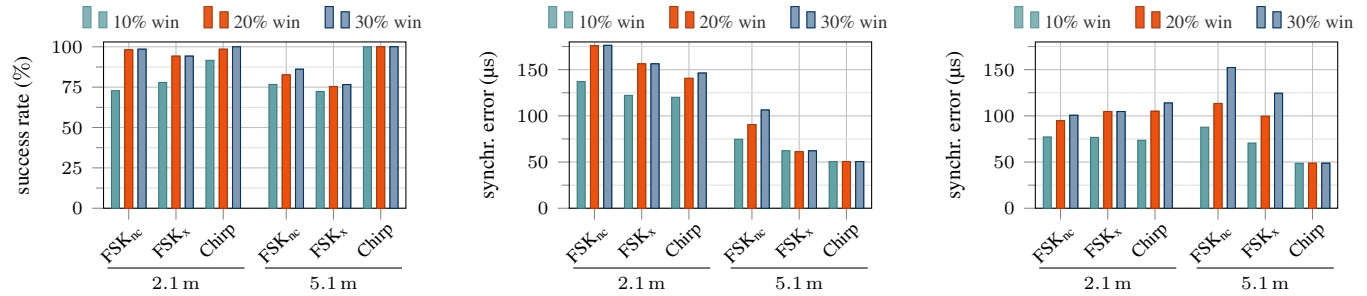

(a) success rate (b) accuracy (c) precision

Fig. 5: Comparison of success rate, accuracy, and precision of synchronization with non-coherent (FSK_{nc}) and cross-correlation (FSK_{x}) vs. chirping. Grouped bars show values for different margins (in percent) w. r. t. symbol length; e.g., a 10% margin is equivalent to 250 µs.

[2] M. Rao, N. K. Kamila, and K. V. Kumar, "Underwater Wireless Sensor Network for Tracking Ships Approaching Harbor," in *Proc. of the IEEE International Conf. on Signal Processing, Communication, Power and Embedded System (SCOPES)*, Oct. 2016.

[3] C. Renner and A. J. Golkowski, "Acoustic Modem for Micro AUVs: Design and Practical Evaluation," in *Proc. of the 11th ACM International Conf. on Underwater Networks & Systems (WUWNet)*, Shanghai, China, Oct. 2016.

[4] E. Gallimore, J. Partan, I. Vaughn, S. Singh, J. Shusta, and L. Freitag, "The WHOI Micromodem-2: A Scalable System for Acoustic Communcations and Networking," in *Proc. of the MTS/IEEE Oceans Conf.*, Sep. 2010.

[5] Evologics GmbH, "Underwater Acoustic Modems," http://www.evologics.de/en/products/acoustics/.

[6] Tritech International Limited, "Micron Data Modem – Acoustic Modem," http://www.tritech.co.uk/product/micron-data-modem.

[7] Teledyne Benthos, "ATM-903 series (OEM)," http://teledynebenthos.com/product/acoustic_modems/903-series-atm-903.

[8] T. Jenserud and S. Ivansson, "Modeling the Power Delay Profile of Underwater Acoustic Channels — The Effects of Out-of-Plane Scattering and Reverberation," in *Proc. of the International Conf. Underwater Communications and Networking (UComms)*, Sestri Levante, Italy, Sep. 2014.

[9] X. Zhao, D. Pompili, and J. Alves, "Energy-efficient OFDM Bandwidth Selection for Underwater Acoustic Carrier Aggregation Systems," in *Proc. of the International Conf. Underwater Communications and Networking (UComms)*, Lerici, Italy, Aug. 2016.

[10] K. Pelekanakis, L. Cazzanti, G. Zappa, and J. Alves, "Decision Tree-based Adaptive Modulation for Underwater Acoustic Communications," in *Proc. of the International Conf. Underwater Communications and Networking (UComms)*, Lerici, Italy, Aug. 2016.

[11] C. Renner, "Packet-Based Ranging with a Low-Power, Low-Cost Acoustic Modem for Micro AUVs," in *Proc. of the 11th International ITG Conf. on Systems, Communications and Coding (SCC)*, Hamburg, Germany, Feb. 2017.

[12] B. Meyer, C. Renner, and E. Maehle, "Versatile Sensor and Communication Expansion Set for the Autonomous Underwater Vehicle MONSUN," in *Proc. of the 19th International Conf. on Climbing and Walking Robots and Support Technologies for Mobile Machines (CLAWAR)*, London, UK, September 2016.

[13] A. Hackbarth, E. Kreuzer, and E. Solowjow, "HippoCampus: A Micro Underwater Vehicle for Swarm Applications," in *Proc. of the IEEE/RSJ International Conf. on Intelligent Robots and Systems (IROS)*, Hamburg, Germany, 2015.